

How Does Ammonium Dynamically Interact with Benzene in Aqueous Media? A First Principle Study Using the Car–Parrinello Molecular Dynamics Method

Rongjian Sa,[†] Weiliang Zhu,^{*,†} Jianhua Shen,^{*,†} Zhen Gong,[†] Jiagao Cheng,[†]
Kaixian Chen,[†] and Hualiang Jiang^{*,†,‡}

Drug Discovery and Design Centre, State Key Laboratory of New Drug Research, Shanghai Institute of Materia Medica, Shanghai Institutes for Biological Sciences, the Graduate School, Chinese Academy of Sciences, 555 Zuchongzhi Road, Shanghai 201203, China, and School of Pharmacy, East China University of Science and Technology, Shanghai 200237, China

Received: April 3, 2005; In Final Form: January 17, 2006

The Car–Parrinello molecular dynamics (CPMD) method was used to study the dynamic characteristics of the cation– π interaction between ammonium and benzene in gaseous and aqueous media. The results obtained from the CPMD calculation on the cation– π complex in the gaseous state were very similar to those calculated from the Gaussian98 program with DFT and MP2 algorithms, demonstrating that CPMD is a valid approach for studying this system. Unlike the interaction in the gaseous state, our 12-ps CPMD simulation showed that the geometry of the complex in aqueous solution changes frequently in terms of the interaction angles and distances. Furthermore, the simulation revealed that the ammonium is constantly oscillating above the benzene plane in an aqueous environment and interacts with benzene mostly through three of its hydrogen atoms. In contrast, the interaction of the cation with the aromatic molecule in the gaseous state involves two hydrogen atoms. In addition, the free energy profile in aqueous solution was studied using constrained CPMD simulations, resulting in a calculated binding free energy of -5.75 kcal/mol at an optimum interaction distance of ~ 3.25 Å, indicating that the cation– π interaction between ammonium and benzene is stable even in aqueous solution. Thus, this CPMD study suggested that the cation– π interaction between an ammonium (group) and an aromatic structure could take place even on surfaces of protein or nucleic acids in solution.

Introduction

The interactions between cations and aromatic systems have attracted much attention in the past two decades in view of their important roles in protein structure as well as their involvement in some biological processes, such as molecular recognition and drug action.^{1–14} The experimental measurements and theoretical calculations of their binding energies demonstrated that the cation– π interaction is generally more extensive than other noncovalent interactions.^{2,11} Some recent studies showed that the interaction between a cation and the π rings of phenylalanine, tyrosine, and tryptophan are common in protein structures.^{3,11} Dougherty and co-workers¹³ used energy-based criteria to search a protein database containing 593 proteins and found that over 25% of all tryptophans possessed an energetically significant cation– π interaction. In another study, Minoux and Chipot³ analyzed a protein database containing 1718 representative structures for the association of phenylalanine, tyrosine, and tryptophan with arginine and lysine and found ~ 2500 cation–aromatic pairs. Thus, the understanding of this interaction would be helpful in elucidating its pivotal role in some biological processes, as well as in aiding new protein design and drug discovery.

Most previous experimental and theoretical studies of the cation– π interaction^{1,2} were focused primarily on the interaction

in the gaseous state rather than in aqueous solution. However, elucidation of these interactions in the aqueous state is important, since most biological processes involving proteins or nucleic acids occur in an aqueous environment. Furthermore, some recent statistics^{12,13} demonstrated that only about 40% of aromatic amino acids tend to be buried within proteins, suggesting that cation– π interaction might occur on the surfaces of proteins. On the other hand, the binding energy between toluene and ammonium is about -17 kcal/mol in the gaseous state, while it is only -2.99 kcal/mol in aqueous solution,¹⁴ suggesting that solvent effects have a profound influence on this interaction. Theoretical studies by Wipff et al.¹⁵ also indicated that the gas-phase binding model between guanidinium ions and benzene is significantly different from that in an aqueous environment. Our previous ab initio computational study revealed that, as water molecules are introduced into the complex of methylammonium–benzene, the binding affinity between the cation and the aromatic ring is significantly weakened.¹⁶ In the light of such data, it is therefore essential to take into account the solvent effect on cation– π interactions. Recently, quantum mechanics (QM) SCRF methods have been increasingly applied to investigate cation– π interactions in aqueous solution. Dougherty and co-workers¹⁷ have adopted the SM5.42R/HF method to investigate cation– π interaction in aqueous media and in a range of organic solvents. Their calculations showed that the interaction energy between methylammonium and benzene in aqueous solution is -5.5 kcal/mol. The classical molecular dynamics (MD) method was also used to explore the cation– π interaction in solvent, such as the interaction between toluene and ammonium.¹⁴ However, there

* Corresponding authors. Please address correspondence and request for reprints to H.J.: phone, +86-21-50807188; fax, +86-21-50807088; e-mail, hljiang@mail.shcnc.ac.cn.

[†] Chinese Academy of Sciences.

[‡] East China University of Science and Technology.

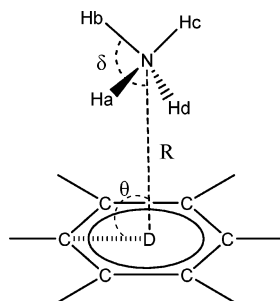


Figure 1. The structure of ammonium–benzene complex. δ is an angle between H*–N and the C6 axis of benzene, R is the N–D distance, θ is an angle of C–D–N, and H* denotes the hydrogen atom of NH₄⁺.

are inherent drawbacks in using MD for characterizing cation– π interaction, as conventional force fields cannot properly describe cation– π interactions in terms of nonelectrostatic interactions, including polarization, dispersion, and charge transfer, between cations and aromatic molecules. Thus, approaches based on quantum mechanics are prerequisite for rigorous and appropriate evaluation of the dynamic characteristics of the interactions. Gao and co-workers¹⁸ performed a QM/MM investigation on the interaction of tetramethylammonium–benzene at the AM1 level, which provided some useful information on this interaction. However, in our experience,^{16,19–26} as well as from the standpoint of data from other publications,^{2,14,17} higher level quantum chemistry methods should be used to obtain reliable and accurate results for the cation– π interaction. Therefore, the Car–Parrinello²⁷ molecular dynamics (CPMD) method at the density functional theory (DFT) level was proposed in this study to simulate the cation– π interaction in aqueous solution.^{28–53} This method has the capability to accurately predict the free energy surface of various chemical reactions^{30–34} and the structures of neutral molecules.³⁵ It has also been recently used to explore ion structures in the aqueous environment.^{36–49} To the best of our knowledge, no first-principle MD simulations have been carried out on the cation– π interaction in the aqueous state to date.

In this study, we performed CPMD calculations with the DFT algorithm on the cation– π complex of ammonium–benzene in both gaseous and aqueous states: (i) to determine the validity of using CPMD for studying the ammonium–benzene system, (ii) to explore the dynamic features of this interaction in aqueous solution, (iii) to predict the binding free energy of ammonium to benzene in aqueous solution, and (iv) to evaluate the possibility for binding between a cationic group and an aromatic group that is exposed to aqueous media.

Computational Details

CPMD Geometrical Optimization in Gaseous State. There are three possible interaction modes between ammonium and benzene in the gas phase: (i) monodentate with one H atom, (ii) bidentate with two H atoms, and (iii) tridentate with three H atoms of ammonium interacting with the benzene ring. QM calculations showed that the bidentate complex is the energetically favored structure among the three models.^{2,19} Thus, our initial model for CPMD simulations was based on the bidentate

structure (Figure 1), which was placed in a cubic cell of 10.0 \times 10.0 \times 10.0 Å³ with periodic boundary conditions. CPMD^{27,54} with the DFT-BLYP (Becke⁵⁵ exchange and Lee–Yang–Parr⁵⁶ correlation) generalized gradient approximation together with the semilocal norm-conserving Troullier Martins⁵⁷ pseudopotentials was adopted for geometrical optimization with the steepest descent and the direct inversion iterative subspace method. This approach has been shown to perform well for hydrogen-bonding systems and liquid structures.^{28–53} The Kohn–Sham orbitals were expanded in plane waves with two different energy cutoffs of 70 and 100 Ry, respectively, to test the effect of the cutoff on the calculated results.

To validate our CPMD results, MP2,⁵⁸ DFT-BLYP, and DFT-B3LYP⁵⁹ methods were employed to optimize the complex and to estimate the binding energies with the 6-31G(d,p) basis set⁶⁰ using the software Gaussian98.⁶¹ The calculated binding energies were corrected for the basis-set superposition error (BSSE). In addition, larger basis sets, e.g., 6-311++G(d,p) for BLYP and B3LYP, were also used for further validation.

CPMD Simulation in Aqueous Solution. The above CPMD-BLYP optimized structure was placed into a cubic supercell (a = 10.5 Å) with 32 water molecules that was created by the software package GROMACS⁶² to mimic an aqueous environment. The computational strategy is the same as that used for gas-phase calculation, but with a cutoff of only 70 Ry. The simulation was performed at 300 K via a Nosé–Hoover thermostat chain.^{63,64} The value of the fictitious electron mass was set to be 1000 au, with an integration time step of 7 au (0.17 fs). The system was equilibrated for 2.7 ps followed by a 9.5 ps simulation for data collection.

Constrained CPMD Simulation. Experimental studies suggested that a positively charged amino moiety tends to approach the face of the aromatic ring axially.^{2,14,19} Thus, the constrained CPMD simulations with an interaction distance R ranging from 2.5 to 7.5 Å and θ = 90.0° (Figure 1) were performed to estimate the binding free energy. The free energy profiles were studied with the Blue Moon ensemble theory. Each sample underwent a 2 ps equilibration time, followed by an additional 0.5 ps simulation for statistical average datum collection. To determine if the binding pattern where the ammonium faces the benzene molecule along the C6 axis is the most favorable interaction mode, we performed a similar constrained CPMD simulation but with θ = 5°. The value of θ was found via CPMD optimization on an initial geometry with R = 8.0 Å by placing the ammonium far away from the C6 axis.

Results and Discussion

Results for the Complex in Gaseous Phase. The calculated geometrical and energetic parameters are very similar among the different methods employed. The largest differences between the results obtained from the Gaussian98 and CPMD calculations were found to be in binding energies (ΔE) and interaction distances (R) (Table 1). Remarkably, the difference in binding energy was less than ± 1.0 kcal/mol, and the deviations in interaction distances was no greater than ± 0.08 Å (Table 1). These observations provided a strong basis to conclude that CPMD is an acceptable approach for studying the NH₄⁺–

TABLE 1: Energetic and Geometrical Parameters Obtained from the Gaussian98 and CPMD Calculations

	BLYP6-31G(d,p)	B3LYP6-31G(d,p)	MP26-31G(d,p)	BLYP6-31++G(d,p)	B3LYP6-31++G(d,p)	CPMD	
						70 Ry cutoff	100 Ry cutoff
R (Å)	2.948	2.944	2.894	2.917	2.958	3.046	3.035
ΔE (kcal/mol)	−16.91	−17.32	−17.41	−15.25	−15.97	−16.32	−15.42

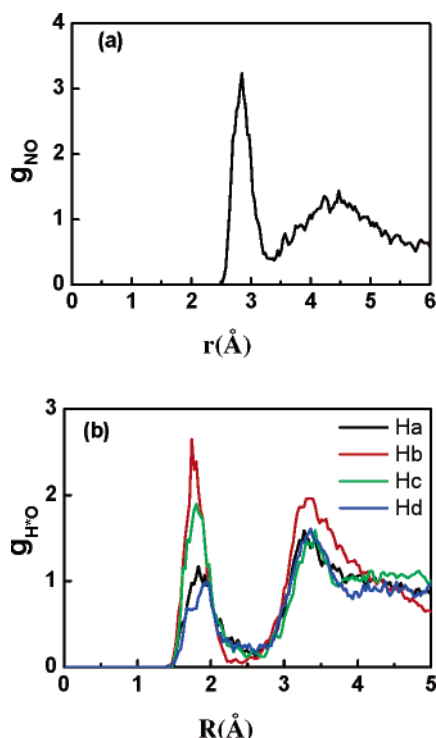


Figure 2. Radial distribution functions for NH_4^+ –benzene in water solution: (a) N–O and (b) H^* –O.

benzene system. Additionally, the data suggested that CPMD with an energy cutoff of 70 Ry was appropriate for calculating both the ΔE and R . Thus, the CPMD method with the energy cutoff of 70 Ry was employed for simulation of the interaction in aqueous solution.

Structural Features in Solution. To characterize the structure of the NH_4^+ –benzene complex in water, radial distribution functions, coordination numbers, interaction distances, and angles of various binding patterns were analyzed on the basis of the 9.5-ps CPMD simulation. Experimental and ab initio molecular dynamic (AIMD) studies suggested that ammonium ions in water possess the coordination number, n_c , of 5.2, as determined by Soper,⁶⁵ and 5.3, as determined by Brüge.⁴⁴ Figure 2a presents the radial distribution of $g_{\text{NO}}(r)$ obtained from our CPMD simulations, which reveals a coordination number of ~ 3.75 by an integration of $g_{\text{NO}}(r)$ for the first solvent shell, demonstrating that the ammonium is not completely hydrated. Thus, the interaction between benzene and ammonium is likely to be responsible for incomplete hydration of the cation. Interestingly, the constrained CPMD simulation also indicated that the four hydrogen atoms of ammonium behaved differently. Figure 2b shows the radial distributions of $g_{\text{HO}^*}(r)$, which demonstrates that the four hydrogen atoms have average coordination numbers of 0.84, 1.01, 1.01, and 0.74, respectively. Figure 3 depicts the distances between the hydrogen atoms and the nearest oxygen atoms along the simulation time, showing that the NH_4^+ tends to form three H-bonds with water in most of the simulation time. Remarkably, while H_b and H_c , which have the same coordination number of 1.01, continuously interact by H-bonding with water molecules for almost all the simulation time, H_a and H_d with the coordination number of 0.84 and 0.74, respectively, intermittently take turns to form hydrogen bonds with water, in a manner akin to these two H atoms of the ammonium playing “rock-and-roll” on the benzene plane. This dynamic interaction pattern is in agreement with the evolution of R and θ along the simulation (Figure 4), which suggests that the interaction between NH_4^+ and benzene is quite

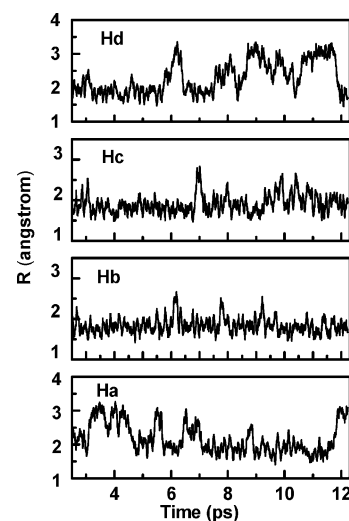


Figure 3. Time dependences of the interaction distances between NH_4^+ hydrogen atoms and the nearest oxygen atoms.

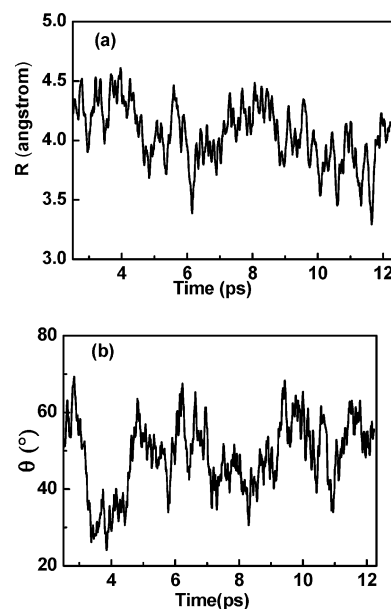


Figure 4. N–D distance R (a) and deviation angle θ (b) versus simulation time.

flexible (refer to Figure 1 for the definitions of R and θ). Therefore, the existence of solvent water molecules leads to a significant change in both the binding pattern and interaction distance between the NH_4^+ and benzene in comparison with the gaseous state, where the interaction is mediated via two H atoms of the cation equidistantly to the benzene.¹⁹

To study the dynamic characteristics of the H atoms of ammonium, an angle δ was defined to monitor the rotation process of the ammonium hydrogen (Figure 1). An ammonium hydrogen atom is directed toward the benzene ring if the angle is less than 90° . It was observed from Figure 5 that the ammonium ion is oscillating above the benzene ring with three of its hydrogen atoms interacting with the benzene ring. Figure 5b depicts the distributions of the three structures, viz., monodentate, bidentate, and tridentate. Noticeably, the tridentate interaction is the most common binding pattern in the aqueous state, accounting for $\sim 63\%$ of total structures, while the bidentate interaction accounts for about 37%. Thus, the monodentate binding is very rare. Therefore, ammonium interacts with benzene in water mostly via three of its hydrogen atoms.

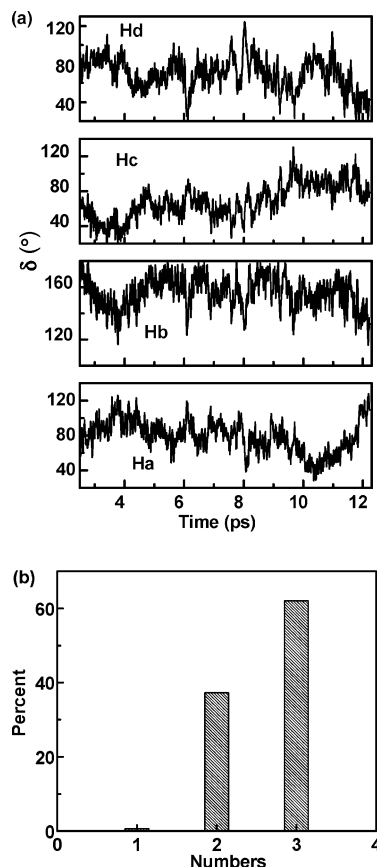


Figure 5. (a) Ammonium hydrogen rotation angle δ (see Figure 1) versus simulation time. (b) Number distribution of ammonium hydrogen atoms toward benzene ring.

To validate the stability of our simulation, the size of the cubic cell, where the NH_4^+ –benzene complex is placed, was increased from $10.5 \times 10.5 \times 10.5 \text{ \AA}^3$ containing 32 water molecules to $15.0 \times 15.0 \times 15.0 \text{ \AA}^3$ containing 108 water molecules. Subsequently, CPMD simulation on the new system was performed using the same parameters as that for the previous. The equilibration time for the new simulation is 1.7 ps followed by data collection for 1 ps. The radial distribution functions of N–O and H–O from the new simulation were found to be very similar to that of the previous simulation (Figures S1 and S2, Supporting Information), showing that the cubic cell size of $10.5 \times 10.5 \times 10.5 \text{ \AA}^3$ is sufficient for studying the dynamic characteristics of the interaction between ammonium and benzene in water. The coordination numbers of N–O and H–O obtained from the new simulation are also almost identical to those from the previous simulation. Therefore, the results obtained from the analyses based on the calculations using the periodic boundary condition of 10.5 \AA should be acceptable.

Free Energy Profile in Aqueous Solution. The free energy profiles calculated by applying constrained CPMD simulations were depicted in Figure 6 for the simulations with $\theta = 90^\circ$ and 5° , respectively.

ΔG from the simulations with the constraint of C6 ($\theta = 90^\circ$) is -5.75 kcal/mol with an optimum interaction distance of 3.25 \AA (Figure 6a). This value agrees well with the experimental result for the complex of Bu_4N^+ –benzene in aqueous media ($\Delta G = -5.5 \text{ kcal/mol}$) by Dougherty et al.¹⁷ and is also consistent with the result from a classical MD simulation of toluene–ammonium by Chipot et al.¹⁴ ($\Delta G = -5.47 \text{ kcal/mol}$). In contrast with the deep and sharp free energy trough depicted in Figure 6a, a broad and flat free energy surface was observed

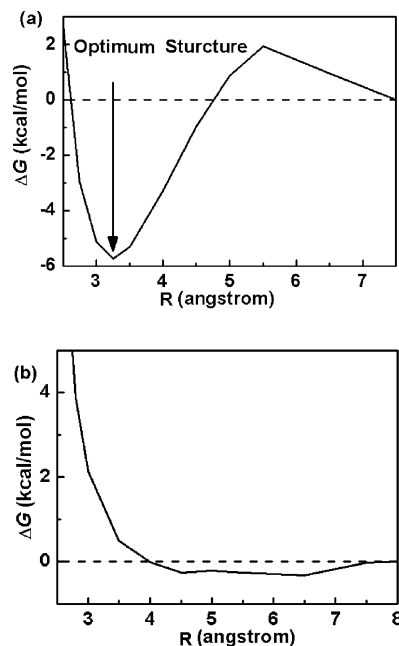


Figure 6. NH_4^+ –benzene free energy profiles in aqueous phase: (a) $\theta = 90^\circ$ and (b) $\theta = 5^\circ$.

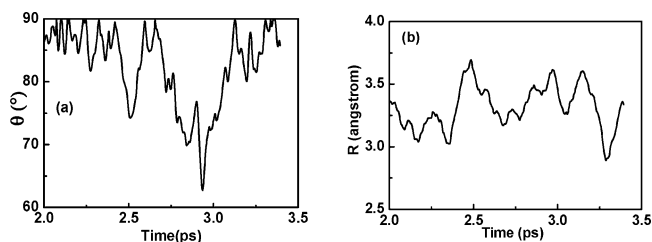


Figure 7. (a) Deviation angle θ variation as a function of simulation time. (b) Time dependence of N–D distance.

with ΔG from -0.16 to -0.33 kcal/mol on the basis of the constrained CPMD simulation with $\theta = 5^\circ$ (Figure 6b). Thus, the two disparate values of ΔG indicate that NH_4^+ prefers to interact with benzene by locating itself above the benzene ring in aqueous solution.

To verify the above postulation, another CPMD simulation was carried out without any structural constraint using the optimum structure with the optimum interaction distance of 3.25 \AA (Figure 6a) as the initial state. The system was equilibrated for 2 ps, followed by data collection for 1.4 ps. Figure 7 shows the evolution of the N–D distance and the deviation angle θ along the simulation time. Clearly, only a few N–D distances are greater than 3.5 \AA , and the θ angle stayed mostly at $\geq 70^\circ$, suggesting that the optimum structure of NH_4^+ –benzene shown in Figure 6a is rather stable. For instance, over 99% of snapshots revealed that the projection of the nitrogen of NH_4^+ is within the benzene ring, supporting our speculation that the NH_4^+ prefers to locate itself above the benzene ring. Taking into account the CPMD-optimized geometry of NH_4^+ – C_6H_6 complex, binding free energy, interaction distance, and the stability of the optimum structure from various CPMD simulations, it is concluded the cation– π binding between ammonium and benzene could exist even in aqueous solution, but this interaction is rather weak and flexible in comparison with that in the gaseous state.¹⁶

Conclusions

Car–Parrinello molecular dynamic simulations were applied to explore the interactions of NH_4^+ interacting with benzene in

water. Our simulations suggested that the CPMD method is capable of reproducing the interaction characteristics with acceptable accuracy for cation- π systems. Radial distribution functions and time-dependent structural analyses revealed that the ammonium ion is not completely hydrated due to its interaction with benzene. However, the estimated interaction distance and free energy change demonstrated that the cation- π interaction is significantly weakened by solvent water molecules. Furthermore, the simulations showed that ammonium continuously oscillates above the benzene ring and interacts with benzene mostly via three of its hydrogen atoms. The binding free energy was estimated to be -5.75 kcal/mol with an optimum distance of 3.25 Å, and this is indicative of a rather strong interaction in comparison with the conventional hydrogen bonding in aqueous solution. Thus, our work provides strong evidence that cation- π interactions could take place even on the surfaces of proteins or nucleic acids in an aqueous environment.

Acknowledgment. We thank Prof. Professor Ursula Röhlisberger, Dr. Jan-Willem Handgraaf, and Dr. Oi Wah Liew for their constructive discussions and suggestions. This work was supported by National Natural Science Foundation (grant 20572117) and the Key Technologies R&D Program of Shanghai (grant 03DZ19228). All the calculations were performed on the supercomputer at Shanghai Supercomputer Center.

Supporting Information Available: Radial distribution functions for N-O in water solution with periodic boundary condition of 15 Å are available in Figure S1, and those for H-O are available in Figure S2. This material is available free of charge via the Internet at <http://pubs.acs.org>.

References and Notes

- (1) Dougherty, D. A. *Science* **1996**, *271*, 163.
- (2) Ma, J. C.; Dougherty, D. A. *Chem. Rev.* **1997**, *97*, 1303. Scrutton, N. S.; Raine, A. R. C. *Biochem. J.* **1996**, *319*, 1. Kim, K. S.; Tarakeshwar, P.; Lee, J. Y. *Chem. Rev.* **2000**, *100*, 4145.
- (3) Minoux, H.; Chipot, C. *J. Am. Chem. Soc.* **1999**, *121*, 10366.
- (4) Fernández-Recio, J.; Vázquez, A.; Civera, C.; Sevilla, P.; Sancho, J. J. *Mol. Biol.* **1997**, *267*, 184.
- (5) Ting, A. Y.; Shin, I.; Lucero, C.; Schultz, G. *J. Am. Chem. Soc.* **1998**, *120*, 7135.
- (6) Doyle, D. A.; Cabral, J. M.; Pfuetschner, R. A.; Kuo, A.; Gulbis, J. M.; Cohen, S. L.; Chait, B. T.; Mackinnon, R. *Science* **1998**, *280*, 69.
- (7) Harel, M.; Schalk, L.; Ehret-Sabatier, L.; Bouet, F.; Goeldner, M.; Hirth, C.; Axelsen, P. H.; Silman, I.; Sussman, J. L. *Proc. Natl. Acad. Sci. U.S.A.* **1993**, *90*, 9031.
- (8) Dougherty, D. A.; Stauffer, D. A. *Science* **1990**, *250*, 1558.
- (9) Deakyn, C. A.; Meot-Ner, M. *J. Am. Chem. Soc.* **1985**, *107*, 474.
- (10) Kumpf, R. A.; Dougherty, D. A. *Science* **1993**, *261*, 1708.
- (11) Zhu, W.; Tan, X.; Puah, C. M.; Gu, J.; Jiang, H.; Chen, K.; Felder, C. E.; Silman, I.; Sussman, J. L. *J. Phys. Chem. A* **2004**, *104*, 9573.
- (12) Gallivan, J. P.; Dougherty, D. A. *J. Am. Chem. Soc.* **2000**, *122*, 870.
- (13) Gallivan, J. P.; Dougherty, D. A. *Proc. Natl. Acad. Sci. U.S.A.* **1999**, *96*, 9459.
- (14) Chipot, C.; Maigret, B.; Pearlman, D. A.; Kollman, P. A. *J. Am. Chem. Soc.* **1996**, *118*, 2998.
- (15) Boudon, S.; Wipff, G.; Maigret, B. *J. Phys. Chem.* **1990**, *94*, 6056.
- (16) Xu, Y.; Shen, J.; Zhu, W.; Luo, X.; Chen, K.; Jiang, H. *J. Phys. Chem. B* **2005**, *109*, 5945.
- (17) Gallivan, J. P.; Dougherty, D. A. *J. Am. Chem. Soc.* **2000**, *122*, 870.
- (18) Gao, J.; Chou, L. W.; Auerbach, A. *Biophys. J.* **1993**, *65*, 43.
- (19) Jiang, H.; Zhu, W.; Tan, X.; Gu, J.; Chen, J.; Lin, M.; Chen, K.; Ji, R. *Sci. China Ser. B, Chem.* **1998**, *41*, 535.
- (20) Zhu, W.; Jiang, H.; Puah, C. M.; Tan, X.; Chen, K.; Cao, Y.; Ji, R. *J. Chem. Soc., Perkin Trans. 2* **1999**, *11*, 2615.
- (21) Zhu, W.; Tan, X.; Puah, C. M.; Gu, J.; Jiang, H.; Chen, K.; Felder, C.; Silman, I.; Sussman, J. L. *J. Phys. Chem. A* **2000**, *104*, 9573.
- (22) Tan, X.; Zhu, W.; Cui, M.; Luo, X.; Gu, J.; Silman, I.; Sussman, J. L.; Jiang, H.; Ji, R.; Chen, K. *Chem. Phys. Lett.* **2001**, *349*, 113.
- (23) Zhu, W.; Puah, C. M.; Tan, X.; Jiang, H.; Chen, K. *J. Phys. Chem. B* **2001**, *105*, 426.
- (24) Zhu, W.; Tan, X.; Shen, J.; Luo, X.; Cheng, F.; Puah, C. M.; Ji, R.; Chen, K.; Jiang, H. *J. Phys. Chem. A* **2003**, *107*, 2296.
- (25) Zhu, W.; Luo, X.; Puah, C. M.; Tan, X.; Shen, J.; Gu, J.; Chen, K.; Jiang, H. *J. Phys. Chem. A* **2004**, *108*, 4008.
- (26) Liu, T.; Zhu, W.; Gu, J.; Shen, J.; Luo, X.; Chen, G.; Puah, C.; Silman, I.; Chen, K.; Sussman, J. L.; Jiang, H. *J. Phys. Chem. A* **2004**, *108*, 9400.
- (27) Car, R.; Parrinello, M. *Phys. Rev. Lett.* **1985**, *55*, 2471.
- (28) Marx, D.; Hutter, J. Ab initio molecular dynamics: Theory and implementation. In *Modern Methods and Algorithms in Quantum Chemistry*; NIC Series Vol. 2; Grotendorst, J., Ed.; NIC: Jülich, Germany, 2000; p 301.
- (29) Carloni, P.; Rothlisberger, U.; Parrinello, M. *Acc. Chem. Res.* **2002**, *35*, 455.
- (30) Carter, E. A.; Ciccotti, G.; Hynes, J. T.; Kapral, R. *Chem. Phys. Lett.* **1989**, *156*, 472.
- (31) Curioni, A.; Sprik, M.; Andreoni, W.; Andreoni, W.; Schiffer, H.; Hutter, J.; Parrinello, M. *J. Am. Chem. Soc.* **1997**, *119*, 7218.
- (32) Boero, M.; Terakura, K.; Tateno, M. *J. Am. Chem. Soc.* **2002**, *124*, 8949.
- (33) Pagliai, M.; Raugei, S.; Cardini, G.; Schettino, V. *J. Mol. Struct. Theochem.* **2003**, *630*, 141.
- (34) Mugnai, M.; Cardini, G.; Schettino, V. *J. Phys. Chem. A* **2003**, *107*, 2540.
- (35) Molteni, C.; Parrinello, M. *J. Am. Chem. Soc.* **1998**, *120*, 2168.
- (36) Tuckerman, M. E.; Laasonen, K.; Sprik, M.; Parrinello, M. *J. Phys. Chem.* **1995**, *99*, 5749.
- (37) Marx, D.; Parrinello, M. *Nature* **1995**, *375*, 216.
- (38) Marx, D.; Parrinello, M. *Science* **1996**, *271*, 179.
- (39) Laasonen, K.; Sprik, M.; Parrinello, M.; Car, R. *J. Chem. Phys.* **1993**, *99*, 9080.
- (40) Rothlisberger, U.; Parrinello, M. *J. Chem. Phys.* **1996**, *106*, 4658.
- (41) Kim, D.; Klein, M. L. *J. Am. Chem. Soc.* **1999**, *121*, 251.
- (42) Laasonen, K.; Klein, M. L. *J. Phys. Chem. Soc.* **1994**, *116*, 620.
- (43) Marx, D.; Tuckerman, M. E.; Hutter, J.; Parrinello, M. *Nature* **1999**, *397*, 601.
- (44) Brue, F.; Bernasconi, M.; Parrinello, M. *J. Am. Chem. Soc.* **1999**, *121*, 10883.
- (45) Buhl, M.; Wipff, G. *J. Am. Chem. Soc.* **2002**, *124*, 4473.
- (46) Leung, K.; Rempe, S. B. *J. Am. Chem. Soc.* **2004**, *126*, 344.
- (47) Spiegel, K.; Rothlisberger, U.; Carloni, P. *J. Phys. Chem. B* **2004**, *108*, 2699.
- (48) Heuft, J. M.; Meijer, E. J. *J. Chem. Phys.* **2003**, *119*, 11788.
- (49) Kuo, I. F. W.; Mundy, C. J. *Science* **2004**, *303*, 658.
- (50) Marx, D.; Sprik, M.; Parrinello, M. *Chem. Phys. Lett.* **1997**, *373*, 360.
- (51) Sprik, M. *J. Phys.: Condens. Matter.* **1996**, *8*, 9405.
- (52) Meijer, E. J.; Sprik, M. *J. Phys. Chem.* **1998**, *102*, 2893.
- (53) Ramaniah, L.; Bernasconi, M.; Parrinello, M. *J. Chem. Phys.* **1999**, *111*, 1587.
- (54) CPMD V3.7, Copyright IBM Corp. 1990–2001, Copyright MPI für Festkörperforschung Stuttgart, 1997–2001.
- (55) Becke, A. D. *Phys. Rev. A* **1988**, *38*, 3098.
- (56) Lee, C.; Yang, W.; Parr, R. G. *Phys. Rev. B* **1988**, *37*, 785.
- (57) Troullier, N.; Martins, J. L. *Phys. Rev. B* **1991**, *43*, 1993.
- (58) Head-Gordon, M.; Pole, J. A.; Frisch, M. J. *Chem. Phys. Lett.* **1988**, *153*, 503. Frisch, M. J.; Head-Gordon, M.; Pople, J. A. *Chem. Phys. Lett.* **1990**, *166*, 275. Head-Gordon, M.; Head-Gordon, T. *Chem. Phys. Lett.* **1994**, *220*, 122. Saebø, S.; Almlöf, J. *Chem. Phys. Lett.* **1989**, *154*, 83.
- (59) Becke, A. D. *J. Chem. Phys.* **1993**, *98*, 5648. Lee, D.; Yang, W.; Parr, R. G. *Phys. Rev. B* **1988**, *37*, 785.
- (60) Hehre, W. J.; Ditchfield, R.; Pople, J. A. *J. Chem. Phys.* **1972**, *56*, 2257.
- (61) Frisch, M. J.; et al. Gaussian 98, revision A.7; Gaussian, Inc.: Pittsburgh, PA, 1998 (Reference S1, Supporting Information).
- (62) Berendsen, H. J. C.; van der Spoel, D.; van Drunen, R. *Comput. Phys. Commun.* **1995**, *95*, 43.
- (63) Nosé, S. *J. Chem. Phys.* **1984**, *81*, 511. Nosé, S. *Mol. Phys.* **1984**, *52*, 255.
- (64) Hoover, W. G. *Phys. Rev. A* **1985**, *31*, 1695.
- (65) Soper, A. K. *J. Chem. Phys.* **1994**, *101*, 6888.